Ab Initio MO Study of Cluster Rearrangements in Pentagonal Pyramidal Clusters: B_6H_{10} Borane and $[(IrB_5H_8)(CO)(PH_3)_2]$ Metallaborane

Alexander M. Mebel,† Keiji Morokuma,*,‡ and Djamaladdin G. Musaev‡

Contribution from the Institute for Molecular Science, Myodaiji, Okazaki 444, Japan, and Cherry L. Emerson Center for Scientific Computation and Department of Chemistry, Emory University, Atlanta, Georgia 30322

Received October 1, 1993. Revised Manuscript Received January 18, 1994®

Abstract: A systematic ab initio molecular orbital (MO) study of nearly all possible degenerate cluster rearrangement mechanisms for B_6H_{10} has been performed at the MP2/6-31G* and the HF/6-31G levels. All the feasible mechanisms have been found to involve an initial diamond–square–diamond (DSD) rearrangement with a high activation energy to form the $B_5H_8(BH_2)$ tetragonal pyramidal intermediate having a bridging BH_2 group. A path from $B_5H_8(BH_2)$ through the middle structure of C_2 symmetry has been shown to be the most favorable for the apical–basal rearrangement. The preferable mechanism for basal–basal reorganization involves scrambling of the bridging BH_2 group from one basal edge to another in $B_5H_8(BH_2)$ and proceeds via the middle structure of nido-type with one square open face. For both mechanisms the initial DSD rearrangement is the rate determining step with the barrier of 47 kcal/mol at the MP2/6-31G*+ZPE level. Any rearrangement mechanism with low activation energy is unlikely to exist. For $[(IrB_5H_8)(CO)(PH_3)_2]$ the isomerization process rearranging the Ir atom from a basal to the apical position is shown to occur by a mechanism similar to that of apical–basal rearrangement of B_6H_{10}. The calculated barrier, 39 kcal/mol at the MP2//HF/ECP-DZ level, is high enough to prevent the isomerization within reasonable temperature.

I. Introduction

Rearrangement mechanisms for borane and heteroborane clusters have been of interest in the chemical literature for several decades. In 1966, Lipscomb first proposed the diamond–square–diamond (DSD) process to account for reorganizations in closo clusters.[1] This mechanism is a cornerstone of many recent theoretical considerations[2-6] of *closo*-boranes and -carboranes including high-level ab initio molecular orbital (MO) calculations of cluster skeleton arrangements in $B_8H_8^{2-}$,[5d,6a] $B_9H_9^{2-}$,[6b] $B_{12}H_{12}^{2-}$, and $C_2B_{10}H_{12}$.[5e] On the other hand, cluster skeleton reorganization mechanisms in nido clusters have been much less explored. For the otherwise deltahedral clusters containing a single square face, Wales and Bone suggested[5d] the so-called square–diamond,-diamond–square (SDDS) mechanism which was shown to be favorable for the $C_5H_5^+$ tetragonal pyramidal cluster. However, for *nido*-boranes, in their opinion, the presence of bridging hydrogen atoms around the open face means that this mechanism is not likely to occur.

Thus, the picture of possible cluster rearrangement mechanisms for *nido*-boranes as well as related carboranes, heteroboranes, and metallaboranes remains unclear. Meanwhile, such rearrangements have been found experimentally. For example, Onak showed the substituted derivative of B_5H_9 pentaborane, *nido*-1,2-$(CH_3)_2B_5H_7$, to rearrange upon heating into the 2,3- and 2,4-isomers.[7] Miller and Grimes, who isolated the 2-isomer of $[(\eta^5\text{-}C_5H_5)CoB_4H_8]$ cobaltaborane, structural and electronic analog of B_5H_9, discovered its thermal rearrangement at 200 °C to the 1-isomer.[8] $[(\eta^5\text{-}C_5H_5)FeB_5H_{10}]$, electronic analog of hexaborane(10), B_6H_{10}, also can exist in two structural forms, 1- and 2-isomers, transforming from one to the other upon temperature change.[9] Only one 2-isomer with the Ir atom in the basal position has been found experimentally for $[(IrB_5H_8)(CO)(PR_3)_2]$ iridaborane,[10] which is also an analog of B_6H_{10}. However, recent ab initio MO calculations of the iridaborane have shown the 1-isomer with apical Ir to be the most stable structure.[11] How the cluster skeleton could rearrange with the metal atom transfer from an equatorial to the axial position and why it does not under experimental conditions are not clear.

As an approach to the study of rearrangement mechanisms in nido clusters, we report here results of systematic calculations of all possible intramolecular mechanisms of cluster skeleton reorganization for B_6H_{10}. The *nido*-hexaborane(10) is found to be nonrigid, and the ^{11}B and ^1H NMR spectra of B_6H_{10} at room temperature are consistent with a pentagonal pyramidal structure, C_{5v}, in solution but only with C_s in the solid state.[12] It has been demonstrated that the fluxionality is due to rapid scrambling of bridging hydrogens. McKee has calculated the barrier for such

† Institute for Molecular Science.
‡ Emory University.
® Abstract published in *Advance ACS Abstracts*, April 1, 1994.

(1) Lipscomb, W. N. *Science* **1966**, *153*, 173.
(2) King, R. B. *Inorg. Chim. Acta* **1981**, *49*, 237.
(3) (a) Gimarc, B. M.; Ott, J. J. *Inorg. Chem.* **1986**, *25*, 2708. (b) Ott, J. J.; Brown, C. A.; Gimarc, B. M. *Inorg. Chem.* **1989**, *28*, 4269. (c) Gimarc, B. M.; Ott, J. J. *Main Group Met. Chem.* **1989**, *12*, 77. (d) Gimarc, B. M.; Daj, B.; Warren, D. S.; Ott, J. J. *J. Am. Chem. Soc.* **1990**, *112*, 2597.
(4) (a) McKee, M. L. *J. Am. Chem. Soc.* **1988**, *110*, 5317. (b) McKee, M. L. *J. Mol. Struct. (THEOCHEM)* **1988**, *168*, 191.
(5) (a) Wales, D. J.; Stone, A. J. *Inorg. Chem.* **1987**, *26*, 3845. (b) Wales, D. J.; Mingos, D. M. P.; Zhenyang, L. *Inorg. Chem.* **1989**, *28*, 2754. (c) Mingos, D. M. P.; Wales, D. J. In *Electron Deficient Boron and Carbon Clusters*; Olah, G. A., Wade, K., Williams, R. E., Eds.; Wiley: New York, 1991; Chapter 5, p 143. (d) Wales, D. J.; Bone, G. A. *J. Am. Chem. Soc.* **1992**, *114*, 5399. (e) Wales, D. J. *J. Am. Chem. Soc.* **1993**, *115*, 1557. (f) Wales, D. J.; Mingos, D. M. P. *Polyhedron* **1989**, *8*, 1933.
(6) (a) Bühl, M.; Mebel, A. M.; Charkin, O. P.; Schleyer, P. v. R. *Inorg. Chem.* **1992**, *31*, 3769. (b) Mebel, A. M.; Charkin, O. P.; Schleyer, P. v. R. *Inorg. Chem.*, submitted.
(7) Tucker, P. M.; Onak, T.; Leach, J. B. *Inorg. Chem.* **1970**, *9*, 1430.
(8) (a) Miller, V. R.; Weiss, R.; Grimes, R. N. *J. Am. Chem. Soc.* **1977**, *99*, 5646. (b) Sneddon, L. G.; Voet, D. *J. Chem. Soc., Chem. Commun.* **1975**, 118. (c) Venable, T. L.; Sinn, E.; Grimes, R. N. *J. Chem. Soc., Dalton Trans.* **1984**, 2275.
(9) (a) Weiss, R.; Grimes, R. N. *J. Am. Chem. Soc.* **1977**, *99*, 8087. (b) Weiss, R.; Grimes, R. N. *Inorg. Chem.* **1979**, *18*, 3291.
(10) Greenwood, N. N.; Kennedy, J. D.; McDonald, W. S.; Reed, D.; Staves, J. *J. Chem. Soc., Dalton Trans.* **1979**, 117.
(11) Mebel, A. M.; Musaev, D. G.; Koga, N.; Morokuma, K. *Bull. Chem. Soc. Jpn.* **1993**, *66*, 3259.
(12) (a) Leach, J. B.; Onak, T.; Spielman, J.; Rietz, R. R.; Schaeffer, R.; Sneddon, L. G. *Inorg. Chem.* **1970**, *9*, 2170. (b) Brice, V. T.; Johnson, H. D., II; Shore, S. G. *J. Chem. Soc., Chem. Commun.* **1972**, 1128. (c) Brice, V. T.; Johnson, H. D., II; Shore, S. G. *J. Am. Chem. Soc.* **1973**, *95*, 6629.

0002-7863/94/1516-3932$04.50/0

a scrambling to be 9.4 kcal/mol at the MP2/6-31G*//SCF/3-21G+ZPE level.[13] On the other hand, there is no experimental evidence of equalizing of all six boron atoms, one apical and five basal, on the NMR time scale. Also, isomerization of the substituted hexaboranyl derivatives has not been observed; rather, decomposition occurs.[14] Hence, the barrier for apical–equatorial cluster rearrangement should be very high. After the study of rearrangements for B_6H_{10}, we present the application of the most favorable mechanism for apical–basal reorganization in the borane to the description of the (1) → (2) isomerization process in the iridaborane, $[(IrB_5H_8)(CO)(PH_3)_2]$.

II. Calculational Methods and Strategy

The rigorous rules which define the allowed symmetries of the transition states for degenerate rearrangements exist only for the maximal symmetry concerted mechanisms where all the common stationary operations are preserved throughout the reaction path.[5f,15] Without any advanced knowledge on the mechanism of degenerate rearrangements of B_6H_{10}, our logical design of nearly all possible pathways is based on the concept of symmetry at the middle points on the potential energy surface. Since we are studying degenerate rearrangements, the potential energy surface on one side of the middle point has to coincide with that on the other side. There are cases in which the critical point at the middle structure is not a stationary point but something like a nonstationary bifurcation point. Excluding these rare cases, there should be some stationary structure in the middle of a pathway, an intermediate or a transition state, in which two exchanging skeleton atoms must be symmetrically equivalent or reflected by a symmetry operation. Therefore, "the middle structure" has to have at least either an axis, a plane, or a center of symmetry, i.e. its the structure has to have symmetry, at least, either C_n, S_n, C_s, or C_i. The procedure for searching nearly all possible rearrangement pathways is as follows: (1) find and select all possible symmetric middle structures and (2) examine the potential energy surface (PES) between middle and ground structures. If some middle structure has one imaginary frequency (number of imaginary frequencies, NIMAG = 1) and is a transition state (TS), we look for the closest minimum using the intrinsic reaction coordinate (IRC) procedure.[16,17] If a middle structure is a minimum (NIMAG = 0), we search for the nearest TS, employing optimization with force constant calculation in every step. The calculation is continued until we reach the global minimum. Since two halves of a rearrangement pathway are equivalent, we had to calculate only one of them.

The preliminary search was carried out at the HF/6-31G level for the middle structures where vibrational frequencies were calculated for characterization and zero-point corrections.[18] All the middle points have been positively identified for equilibrium (NIMAG = 0), transition state (NIMAG = 1), and others. Then, along the paths thus screened, the final search for all the minima and transition states were carried out with electron correlation taken into account at the more reliable MP2(FC)/6-31G* level,[18] where FC denotes frozen core approximation.

In calculations of iridaborane, we used for the Ir atom the Hay–Wadt effective core potential, called ECP17, which takes explicitly into account 17 electrons in $ns np nd(n+1)s(n+1)p$ shells,[19] together with the valence double-ζ [3s3p2d]/(5s5p3d) basis set. The effective core potential (ECP5) was used also for P atoms with the [2s2p]/(3s3p) valence basis set,[20] while for the other nonmetallic atoms, the standard 6-31G basis was employed. We refer this as the ECP-DZ basis set. Geometry optimization was performed at the HF level, which gave satisfactory agreement with experimental X-ray data for the iridaborane,[11] and energies of different structures were recalculated at the MP2 level with HF geometries. All calculations were performed by using the GAUSSIAN92 program.[16]

III. Rearrangements of B_6H_{10}

A. Possible Middle Structures. For the B_6H_{10} cluster, possible minimal symmetry groups within which two boron atoms can be symmetrically equivalent are C_2, C_s, C_i, and C_3. C_5 is not a proper group because there are four additional nonterminal hydrogens in the molecule. $S_1 = C_2$, and $S_2 = C_s$. S_3 does not exist. We characterize each middle structure by the name of the corresponding symmetry group and five integer numbers. The first two numbers refer to the arrangement of boron atoms: (i) the number of B atoms (labeled by R in Figure 1) reflected by the symmetry axis, plane, or center and (ii) the number of borons (labeled by S in Figure 1) located on the symmetry axis or in the symmetry plane. Excluding one hydrogen atom bound on each boron, there are four more hydrogen atoms, and the next three numbers refer to the arrangement of these four hydrogen atoms: (iii) the number of bridging hydrogen atoms (labeled by r in Figure 1) symmetrically equivalent with hydrogens on other B atoms; (iv) the number of hydrogens (labeled by t in Figure 1) symmetrically equivalent with the other hydrogen atom on the same BH_2 group, or the number of BH_2 groups reflected to itself; (v) the number of bridging H's (labeled by s) located on the symmetry axis or in the symmetry plane. For example, $C_s(4,2;2,1,1)$ notation means the structure of C_s symmetry with four B atoms reflected by the symmetry plane, two borons in the plane, two reflecting bridging hydrogens, one symmetric BH_2 group, and one bridging hydrogen on the symmetry plane. We also use $C_s(4,2)$ to represent a family of C_s structures with (4,2) boron arrangement.

The possible arrangements of atoms in B_6H_{10} are shown on Figure 1. In the $C_i(6,0)$ family, six boron atoms could form a distorted octahedron. Only the $C_i(6,0;4,0,0)$ structure is possible within C_i symmetry. Within the $C_2(6,0)$ family, B atoms form a bicapped nonplanar tetragon. $C_2(6,0;4,0,0)$ and $C_2(6,0;2,0,2)$ structures are possible, but the latter is obviously not preferable due to the unfavorable capping position of one hydrogen. In the $C_2(4,2)$ family, again, octahedral disposition of borons could be expected. $C_2(2,4)$ and $C_2(0,6)$ families are not realistic since they would contain too many boron atoms on the same axis. The $C_3(6,0;3,0,1)$ configuration with boron atoms forming a trigonal antiprism would be unfavorable due to the presence of a capping hydrogen and of three H's bridging the edges of the same face. All structures of the $C_s(6,0)$ family can be eliminated because B atoms have to form a trigonal prism, while skeletons of borane clusters are mostly deltahedral.

$C_s(4,2)$ is a set of widely different structures. The borons can form a pentagonal pyramid, a bicapped trapezoid, an octahedron, and chair and bath configurations. Bicapped trapezoids and chair and bath configurations are not interesting for our study; they are not deltahedral clusters. The family of pentagonal pyramidal structures contains the experimental geometry of B_6H_{10}, but they seem to be unimportant as middle structures for degenerate rearrangements of cluster skeleton since they do not contain broken and newly formed B–B bonds as compared with the global minimum. Therefore, we tried to find the middle structures only with initial octahedral disposition of skeletal atoms. For different configurations of $C_s(2,4)$ symmetry, initial location of borons also has been chosen as a distorted octahedron. For the $C_s(2,4)$ family we did not consider configurations with a non-zero number of bridging hydrogens in the symmetry plane because such atoms must be coplanar with terminal H's and disposition of the hydrogens would be too tight.

Thus, we selected as possible candidates for the middle structures the following: $C_i(6,0;4,0,0)$, $C_2(6,0;4,0,0)$, $C_2(4,2;4,0,0)$, $C_2(4,2;2,2,0)$, $C_s(4,2;4,0,0)$, $C_s(4,2;2,0,2)$, $C_s(4,2;2,2,0)$,

(13) McKee, M. L. *J. Phys. Chem.* **1989**, *93*, 3426.
(14) Srivastava, D. K.; Barton, L. *Organometallics* **1993**, *12*, 2864 and references therein.
(15) (a) McIvor, J. W.; Stanton, R. E. *J. Am. Chem. Soc.* **1972**, *94*, 8618. (b) Stanton, R. E.; McIvor, J. W. *J. Am. Chem. Soc.* **1975**, *97*, 3632. (c) Rodger, A.; Schipper, P. E. *Chem. Phys.* **1986**, *107*, 329. (d) Rodger, A.; Schipper, P. E. *J. Phys. Chem.* **1987**, *91*, 189. (e) Rodger, A.; Schipper, P. E. *Inorg. Chem.* **1988**, *27*, 458.
(16) GAUSSIAN92: Frisch, M. J.; Trucks, G. W.; Head-Gordon, M.; Gill, P. M. W.; Wong, M. W.; Foresman, J. B.; Johnson, B. G.; Schlegel, H. B.; Robb, M. A.; Replogle, E. S.; Gomperts, R.; Andres, J. L.; Raghavachari, K.; Binkley, J. S.; Gonzales, C.; Martin, R. L.; Fox, D. J.; DeFrees, D. J.; Baker, J.; Stewart, J. J. P.; Pople, J. A. Gaussian Inc.: Pittsburgh, PA, 1992.
(17) Gonzalez, C.; Schlegel, H. B. *J. Chem. Phys.* **1989**, *90*, 2154.
(18) Hehre, W. J.; Radom, L.; Schleyer, P. v. R.; Pople, J. A. *Ab initio Molecular Orbital Theory*; Wiley: New York, 1986.
(19) Hay, P. J.; Wadt, W. R. *J. Chem. Phys.* **1985**, *82*, 299.
(20) Wadt, W. R.; Hay, P. J. *J. Chem. Phys.* **1985**, *82*, 284.

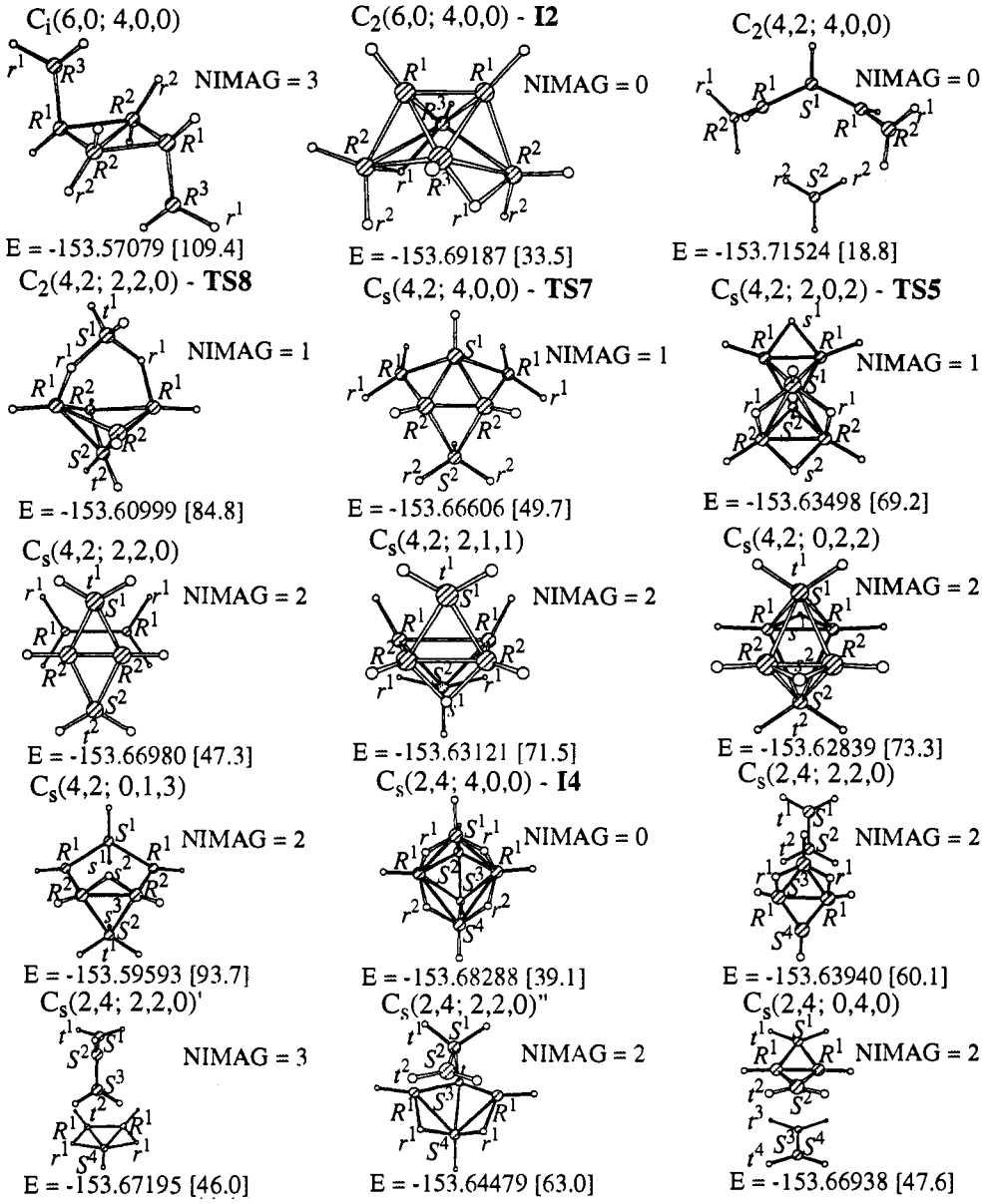

Figure 1. HF/6-31G geometries, total (au) and relative (in brackets, kcal/mol) energies, and number of imaginary frequencies (NIMAG) of possible middle structures for degenerate rearrangements in B_6H_{10}.

$C_s(4,2;2,1,1)$, $C_s(4,2;0,2,2)$, $C_s(4,2;0,1,3)$, $C_s(2,4;4,0,0)$, $C_s(2,4;2,2,0)$, and $C_s(2,4;0,4,0)$. All these structures have been subjected to full geometry optimization within the given symmetry at the HF/6-31G level. The resulting structures, energies, and numbers of imaginary frequencies (NIMAG) are collected in Figure 1. One can see from Figure 1 that the optimized geometries can be quite different from the presumed and above-discussed arrangements of the borons. Initial octahedral geometry is strongly distorted in most cases, and sometimes optimization leads to dissociation of the compound.

Only six among 15 optimized configurations have zero or one imaginary frequency and can, therefore, serve as a middle structure on some degenerate rearrangement pathway. The $C_2(4,2;4,0,0)$ structure is the lowest in energy within this set and lies only 18.8 kcal/mol higher than the global minimum at the HF/6-31G level. However, this configuration corresponds to dissociation of B_6H_{10} to BH_3 and $BH(BHBH_2)_2$. Since we limited our present consideration only to intramolecular rearrangement mechanisms, we did not study the PES between this structure and that at the global minimum. The other five structures, the local minima, $C_2(6,0;4,0,0)$ and $C_s(2,4;4,0,0)$, as well as the transition states, $C_2(4,2;2,2,0)$, $C_s(4,2;4,0,0)$, and $C_s(4,2;2,0,2)$, are the key species of five different rearrangement mechanisms. We denote these mechanisms by the names of the middle structures and discuss them below one by one. Geometries of different minima and transition states, optimized at the more reliable MP2/6-31G* level, are shown in Figure 2, where boron and hydrogen atoms are labeled by numbers and small roman letters, respectively, and the energies are summarized in Table 1. The different mechanisms are presented in Figures 3–7, where dark arrows on the transition structures show the reaction coordinate, i.e. the normal coordinate vector having imaginary frequencies. In the following, all the geometries are optimized at the MP2/6-31G* level, with energies calculated at the same level with the zero-point corrections using the HF/6-31G vibrational frequency scaled by 0.89.[18]

B. The $C_2(6,0;4,0,0)$ Mechanism. At the HF level, the $C_2(6,0;4,0,0)$ middle structure, **I2**, is an intermediate as discussed above. Therefore there must be at least one TS between **I2** and the global minimum (**GM**). The preliminary search at the HF level from **I2** found **TS2'**. An IRC tracing from **TS2'** led to another intermediate, **I1**. Between **I1** and **GM** another TS, **TS1**, was found.

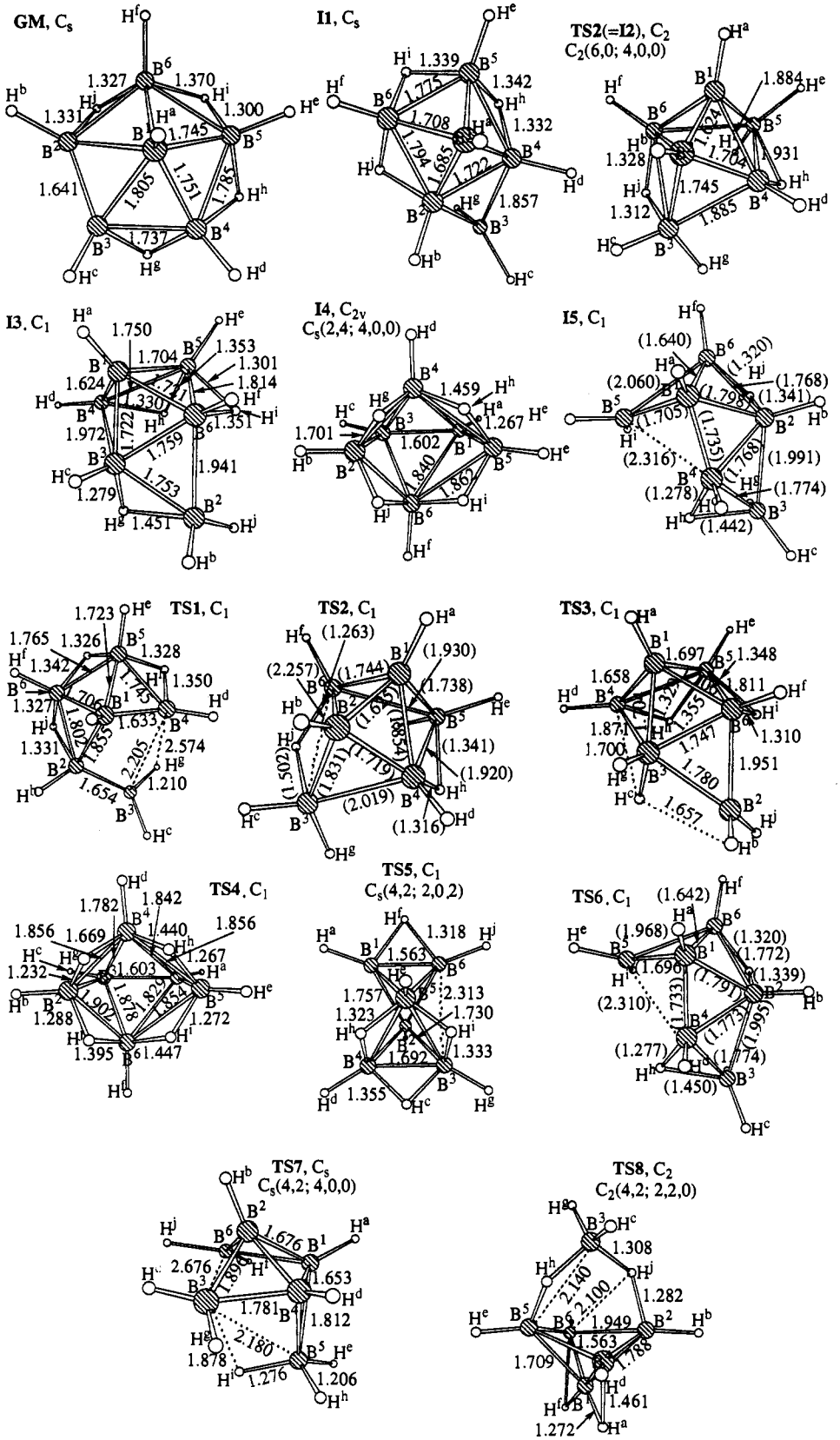

Figure 2. MP2/6-31G* optimized geometries of minima and transition states for B_6H_{10}. For species where only HF/6-31G optimization was done, the values are given in parentheses.

Now we follow the rearrangement mechanism from **GM** through **I2**, at the MP2 level of optimization, as shown in Figure 3. At the first stage, an intermediate **I1** is formed via a transition structure **TS1**. **I1** lies higher than the experimentally observed **GM** by 17.9 kcal/mol at the MP2/6-31G*+ZPE (scaled HF/6-31G) level, at which level all the energies will be reported from here unless otherwise mentioned. The rearrangement is of DSD type; in **I1**, the B^1B^3 bond is broken and the B^2B^4 bond is created as compared with **GM**. At **TS1** B^1, B^2, B^3, and B^4 atoms form an almost planar tetragon with long diagonal B^1B^3 and B^2B^4 distances of 2.75 and 2.41 Å, respectively. Noteworthy, the B^3B^4 bond is also substantially elongated, from 1.74 to 2.21 Å, in **TS1**.

Table 1. Total (au) and Relative (kcal/mol) Energies, Zero-Point Energy Corrections (ZPE, kcal/mol), Number of Imaginary Frequencies (NIMAG), Entropies (cal/(mol·deg)), and Relative Gibbs Free Energies (kcal/mol) Calculated at 298 °C for Minima and Transition States of B_6H_{10}

	HF/6-31G				MP2/6-31G*				
configuration, sym	E_{tot}	E_{rel}	ZPE[a]	NIMAG	E_{tot}	E_{rel}	E_{rel}(with ZPE)[b]	S	ΔG(298 °C)
GM, C_s	−153.745 20	0.0	70.2	0	−154.399 95	0.0	0.0	72.2	0.0
TS1, C_1	−153.697 51	29.9	67.0	1	−154.319 81	50.3	47.1	77.0	45.7
I1, C_s	−153.720 57	15.5	68.0	0	−154.367 93	20.1	17.9	78.7	16.0
TS2', C_1	−153.690 22	34.5	67.3	1	*c*			75.5	
TS2(= I2), C_2	−153.691 87	33.5	67.8	0	−154.339 95	37.7	35.3	75.7	34.3
TS3, C_1	−153.713 81	19.7	67.3	1	−154.361 40	24.2	21.3	75.8	20.1
I3, C_1	−153.714 30	19.4	68.1	0	−154.362 57	23.5	21.4	76.2	20.2
TS4, C_1	−153.682 69	39.2	67.8	1	−154.340 59	37.3	34.9	74.0	34.4
I4, $C_s \rightarrow C_{2v}$	−153.682 88	39.1	68.0	0	−154.340 98	37.0	34.8	75.5	33.8
TS5, C_s	−153.634 98	69.2	66.8	1	−154.302 94	60.9	57.5	75.7	56.5
TS6, C_1	−153.712 60	20.5	67.8	1	*c*			77.9	
I5, C_1	−153.713 03	20.2	67.8	0	*c*			78.0	
TS7, C_s	−153.666 06	49.7	65.1	1	−154.284 10	74.4	69.3	81.9	66.4
TS8, C_2	−153.609 99	84.8	65.7	1	−154.261 41	86.9	82.4	76.6	81.1

[a] ZPE scaled by 0.89 as recommended in ref 18. [b] Relative energies at the MP2/6-31G*+ZPE (scaled HF/6-31G) level. [c] The structures are not stationary points at the MP2/6-31G* level.

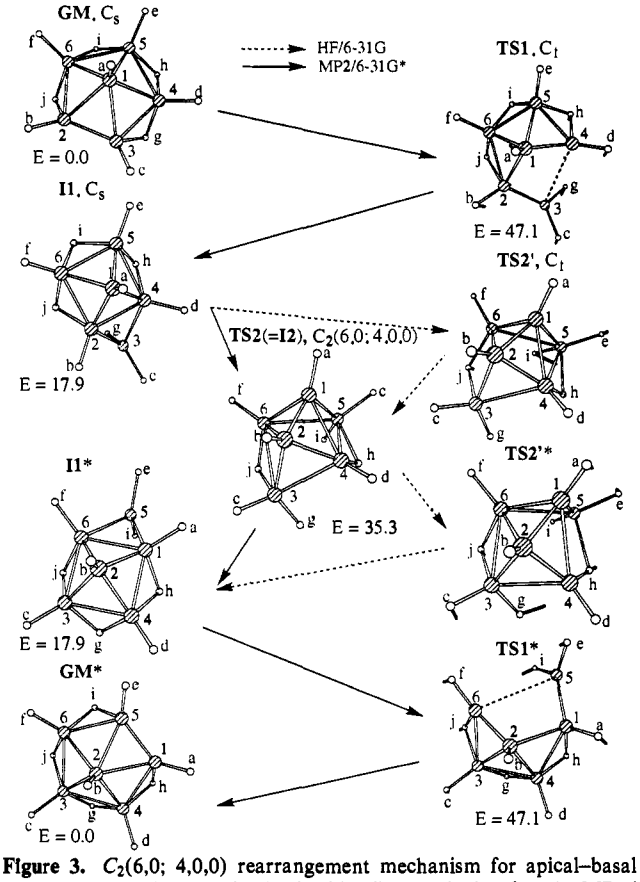

Figure 3. C_2(6,0; 4,0,0) rearrangement mechanism for apical–basal exchange. Relative energies (E, kcal/mol) are calculated at the MP2/6-31G*+ZPE level.

The transition state has a high energy with the barrier of 47.1 kcal/mol. The geometric structure of **I1** (C_s) can be described as $B_5H_8(BH_2)$, e.g. a square pyramidal B_5H_9 cluster with a BH_2 group replacing a bridging hydrogen.

An orbital crossing for DSD rearrangements generally results if a mirror plane through the critical face is retained throughout the process which is therefore symmetry forbidden. If a C_2 axis is retained, then there is an avoided crossing and the process is allowed.[5] Neither a symmetry plane nor a symmetry axis are retained throughout the **GM** → **TS1** → **I1** DSD rearrangement. Hence, it would be difficult to characterize this process a priori as "forbidden" or "allowed". Moreover, none of the symmetry operations of **GM** are maintained during the whole rearrangement process and all our calculations between the middle structures and **GM** have been performed under C_1 symmetry constraints, making all the processes formally "allowed".

From **I1** the rearrangement proceeds by movement of the B^3 atom toward B^6. In **I2**, the middle structure of the C_2(6,0; 4,0,0) pathway, the B^3B^6 bond is formed and H^j becomes a bridging hydrogen between B^3 and B^6. The B^2 atom is pushed up from the pyramidal base; the nonplanar equatorial area of the polyhedron includes B^3, B^4, B^5, and B^6 atoms, and B^1 and B^2 occupy two capping positions. The H^i hydrogen leaves the B^5B^6 bridging position and in **I2** is bound only with B^5 to form a BH_2 group. At the HF/6-31G level, **I2** has no imaginary frequencies and is separated from **I1** by a late transition state, **TS2'**, which has the structure and energy both close to those of **I2**. However, optimization of **TS2'** at the MP2/6-31G* level converges to the structure of C_2 symmetry, equivalent with **I2**. Hence, at this higher level of theory, **I2** is not an intermediate but is a transition structure for **I1** → **I1*** reorganization. From here on, we rename **I2** as **TS2**. The final energy of **TS2** in our best approximation is 35.3 kcal/mol; it is significantly lower than that of **TS1**.

In **TS2** the pairs B^1 and B^2, B^3 and B^5, and B^4 and B^6 are symmetrical and the structures through the second part of the rearrangement pathway can be obtained by 180° rotation around the vertical C_2 axis. The **TS2** transition state transforms into the **I1*** intermediate, which has B^5 in the bridging position between B^1 and B^6, with H^h on the B^1B^4 bond; B^1, B^4, B^3, and B^6 form the base of a tetragonal pyramid, and B^2 occupies the apical position. Then, again, a DSD rearrangement takes place, **I1*** → **TS1*** → **GM**. The B^1B^6 bond is broken, and the B^2B^5 bond is formed. Thus, the system returns to the global minimum, a pentagonal pyramid with four bridging hydrogens around the base, but the axial B^1 and the equatorial B^2 atoms together with corresponding hydrogens have been exchanged, as well as B^3 and B^5, B^4 and B^6, H^i and H^g, and H^j with H^h.

The overall pathway of the degenerate rearrangement is **GM** → **TS1** → **I1** → **TS2** → **I1*** → **TS1*** → **GM***, and the largest barrier, 47.1 kcal/mol, corresponds to **TS1** and **TS1***. Such a scrambling might render all boron atoms equivalent on the NMR time scale, but the barrier is too high, much higher than that of bridging hydrogen scrambling equalizing only the basal borons. During the rearrangement, the number of B–B connections gradually increases for B^2, it has three skeleton neighbors in **GM** and **TS1**, four neighbors **I1**, **TS2**, **I1***, and **TS1***, and five adjacent borons in **GM***. On the contrary, the frame coordination number gradually declines for B^1, from five in **GM**, to four in **TS1**, **I1**, **TS2**, and **I1***, and to three in **TS1*** and **GM***. B^2 loses its bridging hydrogen in **TS2**, and B^1 acquires a bridge in **I1***.

C. The C_s(2,4; 4,0,0) Mechanism. As seen in Figure 4, the first step of the rearrangement with the C_s(2,4; 4,0,0) middle

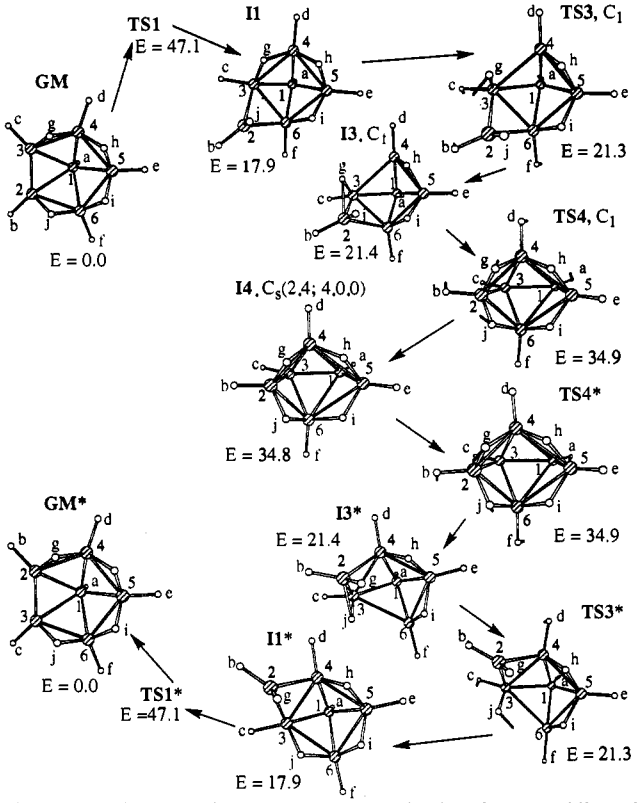

Figure 4. C_s(2,4; 4,0,0) rearrangement mechanism for scrambling of basal atoms. Relative energies (E, kcal/mol) are calculated at the MP2/6-31G*+ZPE level.

point coincides with that of the C_2(6,0; 4,0,0) mechanism; the **I1** intermediate forms after overcoming the **TS1** barrier. Then, scrambling of the bridging H^g hydrogen takes place. H^g, bridging between B^3 and B^4 in **I1**, becomes a member of the B^3H_2 group in **TS3** and moves to the bridging position between B^2 and B^3 in **I3**. The barrier for this hydrogen migration is low, **TS3** lying only 3.4 kcal/mol above **I1**. **I3** and **TS3** are very close in energy; without ZPE **TS3** is 0.7 kcal/mol higher, but with ZPE **TS3** becomes 0.1 kcal/mol more stable than the intermediate. This means that **I3** is not a thermodynamic intermediate and that the reaction should proceed further without stopping at **I3**.

The skeleton reorganization from **I3** to **I4** proceed by motion of B^2 in the direction toward B^4. In **I4**, the C_s(2,4; 4,0,0) middle structure and intermediate, the new B^2B^4 bond is created, H^g is located in a bridging position between B^2 and B^4, and H^j, a member of the B^2H_2 group in **I3**, now bridges the B^2B^6 bond. The transition structure from **I3** to **I4**, **TS4**, is a late TS and has a geometry and an energy both similar to those of **I4**. **I4** is 34.9 and 17.0 kcal/mol less stable than **GM** and **I1**, respectively. The intermediate **I4** is only 0.1 kcal/mol more stable than **TS4** and **TS4***, suggesting again that the reaction will proceed without stopping at **I4**. The geometry of **I4** is noteworthy. This structure, possessing C_{2v} symmetry and called an "envelope structure", represents the second possible nido configuration which can be formed by six skeletal atoms.[21] While for B_6H_{10} such a structure appears to be an unstable intermediate, a similar configuration has been observed experimentally, for example, for $B_4H_4N_2(t\text{-}Bu)_2$ *nido*-azaborane[22] and for $S_2B_2(CpCo)_2$.[23]

The second half of the rearrangement pathway is a mirror reflection of the first half by the horizontal plane. From **I4** to **I3*** via **TS4***, the B^2B^6 bond is broken, H^j moves from the B^2B^6 to the B^2B^3 bridge, and H^g becomes a terminal hydrogen involved in the B^2H_2 group. Then, along the **I3*** → **TS3*** → **I1*** part of the PES, H^j scrambles into the B^3B^6 bridging position. In **I1***, B^2 is again in a bridging location, this time at the B^3B^4 basal edge of the tetragonal pyramid. One of the B^2 bridging hydrogens, H^j, has been replaced by H^g. A DSD rearrangement, **I1*** → **TS1*** → **GM**, returns the system to the global minimum; the B^1B^2 is created perpendicular to the B^3B^4 bond which was broken, and H^g is located in the bridging position between B^2 and B^4.

Interestingly, after the overall rearrangement, only B^2 and B^3 atoms together with the corresponding terminal hydrogens, H^b and H^c, exchange their positions; the other atoms including the apical B^1 remain at the original places. Thus, this mechanism causes reorganization of equatorial atoms but not an apical–basal rearrangement. Since two adjacent basal atoms are exchanged in the C_s(2,4; 4,0,0) rearrangement, a set of similar sequential reorganizations can lead to any possible order of the atoms in the cluster base. It is also conceivable that directly from **I1***, not going down to **GM***, another scrambling takes place via **I1*** → **I4*** → ··· → **I1**** → **GM**** pathway, where in **I1****, B^2 would occupy a bridging position between B^4 and B^5, and in **GM****, B^2 would be shifted two positions in the base compared with the original position in **GM**. Sequential rearrangements of the **I1** → **I1*** → **I1**** type thus can lead the B^2 atom to any equatorial position.

The motif described here for the C_s(2,4; 4,0,0) rearrangement seems to be applicable to basal–basal reorganizations not only in a pentagonal pyramidal cluster but also in other nido clusters. It includes a DSD rearrangement with one equatorial atom scrambling from a cage into a bridging position near a basal edge as the first step. The aperture of the cluster decreases. Then, this atom can migrate from one bridging position to another. Finally, the bridging heavy atom occupies some other equatorial place by the reversal of the DSD mechanism.

An interesting aspect concerning the energetics for the present C_s(2,4; 4,0,0) rearrangement pathway is that the highest barrier, 47.1 kcal/mol, corresponds to the initial **GM** → **TS1** step, the same one that is rate determining in the preceding C_2(6,0; 4,0,0) rearrangement. Another interesting point is that the barrier for the succeeding steps in the present rearrangement, 34.9 kcal/mol, is very similar to that for the C_2(6,0; 4,0,0) rearrangement. These results imply that once the first barrier is cleared, both rearrangement processes can proceed rather easily.

D. The C_s(4,2; 2,0,2) Mechanism. The intermediate **I1** can be subjected to degenerate rearrangement by another way, i.e. via **TS5**, the C_s(4,2; 2,0,2) middle structure, as shown in Figure 5. On going from **I1** to **TS5**, the B^1B^4 bond is broken and the B^3B^5 bond is formed. The $B^2B^4B^3$ triangle moves and turns in such a way that B^3 approaches B^5 and B^4 goes away from B^1. The changes in the boron cage are accompanied by four hydrogen migrations. The terminal H^f atom of B^6 in **I1** moves to a bridging position between B^1 and B^6 in **TS5**, and H^i which bridged B^2B^6 replaces H^f in the B^6 terminal position. The terminal H^c on B^3 becomes a B^3B^4 bridging hydrogen, while the H^i hydrogen scrambles from the B^5B^6 edge to bridge the newly created B^5B^3 bond. The transition state **TS5** lies 39.6 and 57.5 kcal/mol above **I1** and **GM**, respectively.

Boron atom disposition in **TS5** resembles an octahedron, but the B^1B^4 and the B^3B^6 distances are long and nonbonding, 2.31 Å at the MP2/6-31G* level. Hence, **TS5** is not a closo structure. The configuration has a vertical plane of symmetry; B^1 and B^6 atoms, as well as B^3 and B^4, are reflected by this plane. From **TS5** to **I1***, the $B^2B^4B^3$ triangle turns further, and the B^3B^6 bond is created, while the B^4B^5 bond is broken. H^c together with H^d forms a BH_2 group with B^4, and H^h transfers from B^4B^5 into the B^5B^1 bridging position. H^a becomes a bridging hydrogen between B^1 and B^2, and H^f occupies its terminal place near B^1. As

(21) (a) Williams, R. E. In *Electron Deficient Boron and Carbon Clusters*; Olah, G. A., Wade, K., Williams, R. E., Eds.; Wiley: New York, 1991; Chapter 2, p 11. (b) Williams, R. E. *Chem. Rev.* **1992**, *92*, 177.

(22) Paetzold, P. In *Boron Chemistry*; Hermanek, S., Ed.; World Sci. Publ. Inc.: Singapore, 1987.

(23) Kang, S. O.; Sneddon, L. G. *Inorg. Chem.* **1988**, *27*, 3769.

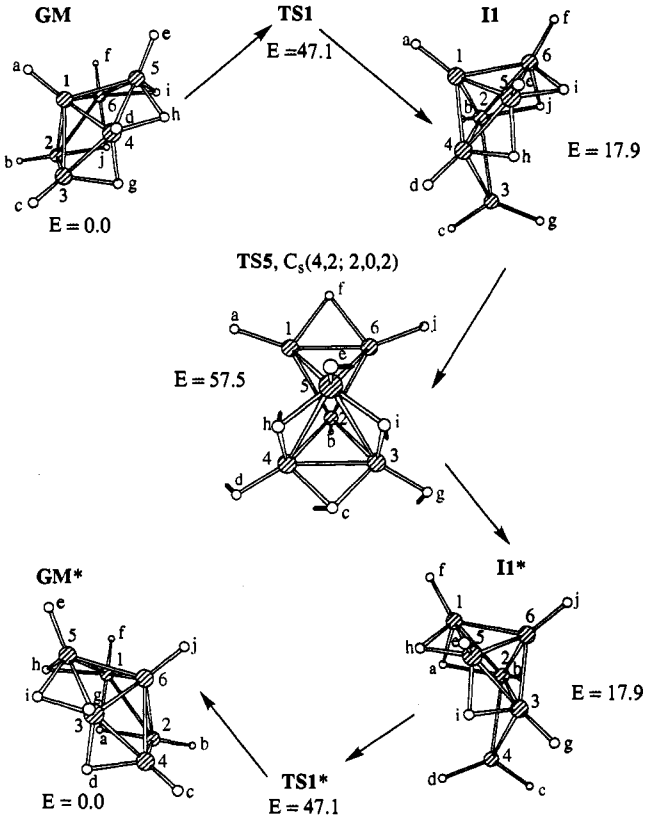

Figure 5. C_s(4,2; 2,0,2) rearrangement mechanism for exchange of basal and apical atoms and two basal atoms. Relative energies (E, kcal/mol) are calculated at the MP2/6-31G*+ZPE level.

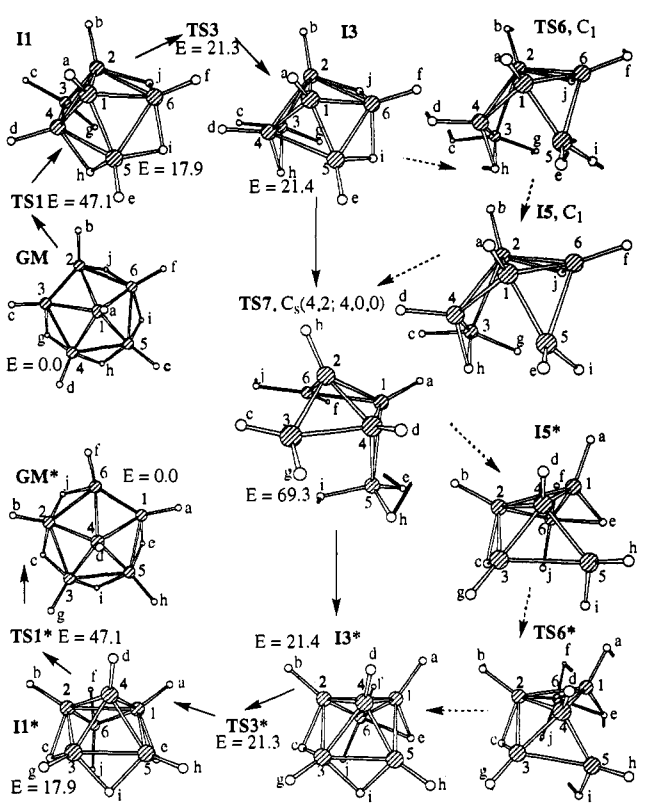

Figure 6. C_s(4,2; 4,0,0) rearrangement mechanism for exchange of basal and apical atoms and two basal atoms. Relative energies (E, kcal/mol) are calculated at the MP2/6-31G*+ZPE level. Broken arrows indicate the HF pathway.

compared with in **I1**, in **I1***, B^6 is the apical atom instead of B^1, and B^4 bridges the B^2B^3 bond instead of B^3 bridging the B^2B^4 bond.

The overall C_s(4,2; 2,0,2) mechanism starts and finishes with the DSD rearrangements, **GM** → **TS1** → **I1** and **I1*** → **TS1*** → **GM***, common to all the three overall mechanisms discussed so far. In going from **GM** to **GM*** by this mechanism, the following atoms have exchanged positions: apical B^1 with equatorial B^6, basal B^3 with basal B^4 atoms, apical terminal H^a with bridging H^i, terminal H^d with bridging H^g, and bridging H^h with bridging H^i. All these pairs of atoms reflect each other by the symmetry plane in **TS5**, the middle structure. The atoms which lie in the plane in **TS5**, namely, B^2, B^5, H^b, H^e, H^c, and H^f, do not change their positions in going from **GM** to **GM***. The highest point on the rearrangement pathway corresponds to **TS5**, and its energy, 57.5 kcal/mol, is higher than that of **TS1** for the initial DSD reorganization.

E. The C_s(4,2; 4,0,0) Mechanism. The first steps of this mechanism up to the formation of the **I3** intermediate coincide with those of the C_s(2,4; 4,0,0) rearrangement in Figure 4. However, as seen in Figure 6, degenerate **I3** → **I3*** reorganization here takes place via **TS7**, the C_s(4,2; 4,0,0) middle structure. The main component of the **I3** → **TS7** → **I3*** scrambling is movement of B^5 from the bonding position with B^6 to that with B^3. In **TS7**, the B^5B^6 bond is broken, and in **I3***, the new B^5B^3 bond is created. Several bridging hydrogens also migrate. H^i transfers from the B^5B^6 bridging position in **I3** to a capping location in **TS7**, where it is strongly bound to B^5 with a bond distance of 1.28 Å and weakly bound with B^3 and B^6 with the bond distances of 1.88 Å. Then it moves into the B^5B^3 bridging position in **I3***. H^h, B^3B^4 bridging in **I3**, becomes a terminal hydrogen of B^5 in **TS7** and remains there in **I3***. Correspondingly, H^e, terminal on B^5 in **I3** and **TS7**, bridges the B^1B^6 bond in **I3***. Thus, B^5 serves as the pivot for transfer of three hydrogen atoms. Meanwhile, the bridging B^2B^6 hydrogen H^j in **I3** becomes terminal on B^6 in **TS7** and, correspondingly, the terminal H^c on B^3 in **I3** and **TS7** occupies a B^2B^3 bridging position in **I3***.

The B^3–B^6 pair as well as the B^1–B^4 pair, symmetrical in **TS7**, exchanges its position during the **I3** → **TS7** → **I3*** rearrangement. B^1 in the apical position in **I3** is replaced by B^4 in **I3***. B^3 in the bridging position in **I3** is substituted by B^6 in **I3***. If one compares **GM** and **GM***, one can see that the following exchanges have taken place: B^1 and B^4 accompanying their terminal hydrogens, H^a and H^d, B^3 and B^6, H^j and H^c, H^g and H^f, and H^e and H^h. B^2, H^b, B^5, and H^i remain in the same places. The geometry of **TS7** is rather of arachno-type, and one of the boron atoms, B^5, is connected with three hydrogens. This makes **TS7** very high in energy, 47.9 kcal/mol above **I3** or 69.3 kcal/mol relative to **GM**. Hence, this C_s(4,2; 4,0,0) mechanism, providing the exchange between the apical and a basal boron as well as between two equatorial atoms, is less favorable to the previous C_s(4,2; 2,0,2) mechanism giving the same exchanges.

On the PES calculated by the HF/6-31G method, there exist two additional stationary points between **I3** and **TS7**. The **I5** intermediate differs from **I3** by absence of the B^5B^4 bond and the location of H^i. **I5** is higher than **I3** by 0.8 kcal/mol at the HF/6-31G level and separated from the latter by a small barrier of 0.3 kcal/mol at the transition structure **TS6**, the geometry of which is close to that of **I5**. However, at the higher MP2/6-31G* level of optimization, **I5** and **TS6** disappear and **I3** is connected directly to **TS7**.

F. The C_2(4,2; 2,2,0) Mechanism. The last possible mechanism, with the C_2(4,2; 2,2,0) middle structure as shown in Figure 7, resembles C_s(2,4; 4,0,0) and C_s(4,2; 4,0,0) rearrangements shown in Figures 4 and 6, respectively, in the sense that they all proceed through the intermediate **I3** which is formed from **GM** via the intermediate **I1**. In this mechanism, **I3** is transformed into **I3*** via the transition state **TS8**. **TS8** corresponds to a barrier for scrambling of the B^3 bridging boron from the B^2B^4 edge to the B^5B^6 edge. At the transition state the B^3B^4 bond is broken

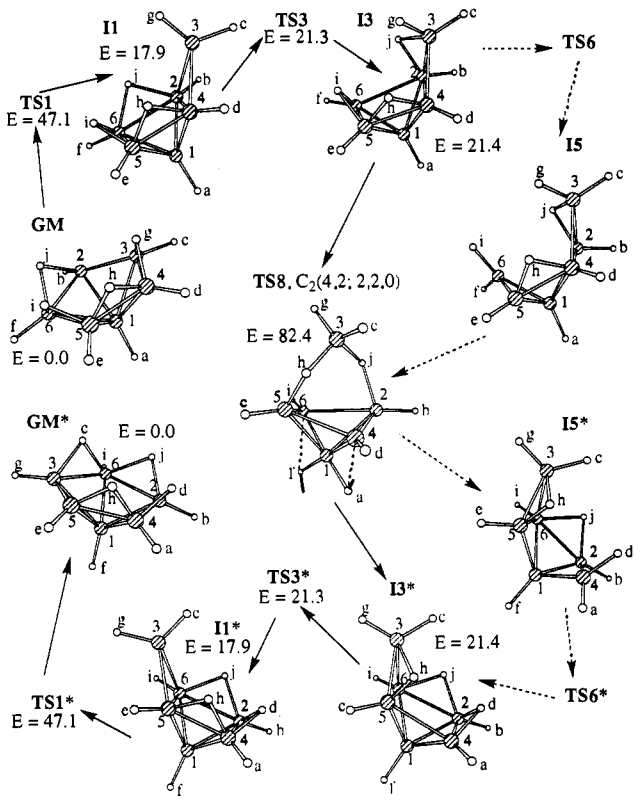

Figure 7. C_2(4,2; 2,2,0) rearrangement mechanism for scrambling of basal atoms. Relative energies (E, kcal/mol) are calculated at the MP2/6-31G*+ZPE level. Broken arrows indicate the HF pathway.

and the B^3B^2 bond is stretched significantly, to 2.14 Å. The B^3B^5 distance becomes the same as the B^3B^2 distance, indicating the new bond formation. H^h, which used to bridge B^5B^4 in **I3**, now bridges B^5B^3 in **TS8**. Additionally, H^f migrates from B^6 to the B^1B^6 bond, and H^i follows it from B^5B^6 to B^6, pushing H^a from B^1 to a B^1B^4 bridging location. In **I3***, the new B^3B^5 bond becomes stronger and another new B^3B^6 is created, H^j moves from B^2B^3 to B^2B^6, the H^d hydrogen is pushed from B^4 into a B^2B^4 bridging position by H^a, which moves from B^1B^4 to a terminal position at B^f, and consequently H^f from B^1B^6 gets to the apical terminal position at B^1.

As compared with **GM**, in **GM***, the pairs of H^f and H^a, H^h and H^j, and H^g and H^c hydrogen atoms have been exchanged. B^3 migrates from an equatorial position between B^2 and B^4 in **GM** to another equatorial position between B^5 and B^6 in **GM***. Hence, the mechanism corresponds to the rearrangement within basal skeletal atoms and does not exchange the apical boron. However, different from the C_s(2,4; 4,0,0) mechanism, this rearrangement involves the axial terminal hydrogen which exchanges with a basal terminal H.

The overall barrier for this C_2(4,2; 2,2,0) mechanism is the highest of all the mechanisms studied, 82.4 kcal/mol at **TS8**. **TS8** lies higher than **I4** and **TS4** by about 50 kcal/mol; migration of the bridging boron onto the adjacent basal edge is much easier than the scrambling onto the opposite edge. At the HF/6-31G level, again, **TS6** and **I5** were found between **I3** and **TS8** but disappeared when electron correlation was taken in to account.

G. Overall Picture of Degenerate Skeleton Rearrangements in B_6H_{10}. The overall potential energy profile for the **GM** → **GM*** degenerate skeleton rearrangement of B_6H_{10} is summarized in Figure 8. As seen in Table 1, differences in entropy values are quite small for the calculated minima and transition states. Therefore, the relative order of the Gibbs free energies, i.e., the relative ease of reaction among various mechanisms, is not likely to change with the temperature. As seen in Figure 8, all the mechanisms have to start with the DSD reorganization, **GM** →

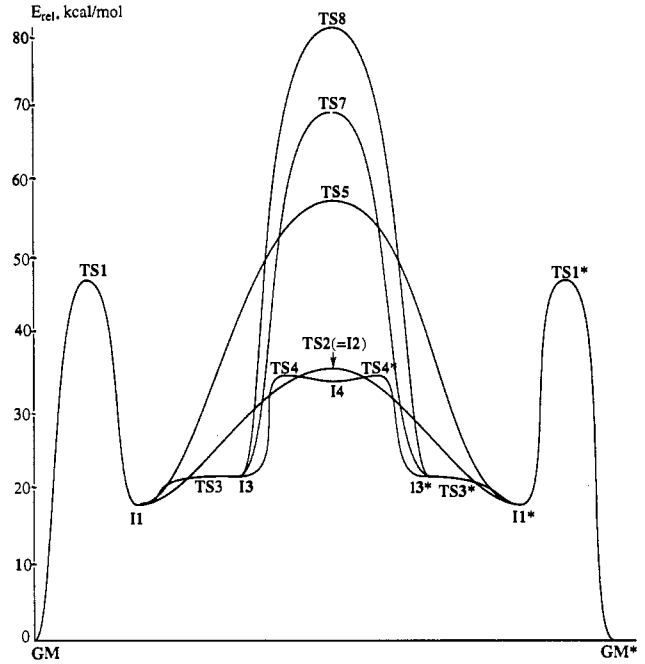

Figure 8. Overall potential energy profiles for the **GM** → **GM*** degenerate skeleton rearrangements of B_6H_{10} at the MP2/6-31G*+ZPE level.

TS1 → **I1**; **I1** can be considered to be the active intermediate for any mechanism of skeleton rearrangement. The activation barrier of 47.1 kcal/mol is very high, and therefore, such rearrangements are expected to require an elevated temperature for this cluster. Once **I1** is formed, the succeeding processes can occur relatively easily. A direct conversion of **I1** to an equivalent **I1*** can take place most easily via **TS2** by the C_2(6,0; 4,0,0) mechanism or less easily via **TS5** by the C_s(4,2; 2,0,2) mechanism. Otherwise, **I1** might be converted to the second common intermediate **I3** relatively easily. Then **I3** → **I3*** scrambling can go by three different ways, most easily via **TS4** and **I4** in the C_s(2,4; 4,0,0) mechanism and much less easily either via **TS7** in the C_s(4,2; 4,0,0) mechanism or via **TS8** in the C_2(4,2; 2,2,0) mechanism.

Two low energy mechanisms, C_2(6,0; 4,0,0) via **TS2** and C_s(2,4; 4,0,0) via **TS3** → **I3** → **TS4** → **I4**, with DSD scrambling are the most important for apical–basal rearrangements and for reorganizations within the base, respectively. The C_s(4,2; 2,0,2) mechanism via **TS5**, though requiring a high energy, is interesting because it involves remarkable exchanges of almost all hydrogen atoms besides the apical–basal and basal–basal skeleton scrambling. Such a mechanism might be important for isomerization in clusters where some bridging or terminal hydrogens are substituted by other ligands, e.g. for axial–equatorial or terminal–bridging exchange of different ligands.

IV. Mechanism of (2) → (1) Isomerization in $[(IrB_5H_8)(CO)(PH_3)_2]$

Several alternative isomers differing by the position of the Ir atom in the cluster skeleton and by arrangement of the bridging hydrogens were calculated earlier[11] for $[(IrB_5H_8)(CO)PH_3)_2]$. Their geometries and MP2//HF/ECP-DZ relative energies are shown in Figure 9. In the configurations (1) and (1a), the Ir atom is situated in the apical position. In (1a) three bridging hydrogens are adjacent, and in (1) two are adjacent and one is isolated. For each of (1) and (1a), two conformations are possible, with CO and B^1 ligands on the metal atom to be in a "trans" or "cis" position, but they are similar in energy. In the isomers (2) and (3), Ir is located in the basal position, and one of the additional hydrogens is connected only with Ir. In (3) two remaining bridges are adjacent, and in (2) they are separated.

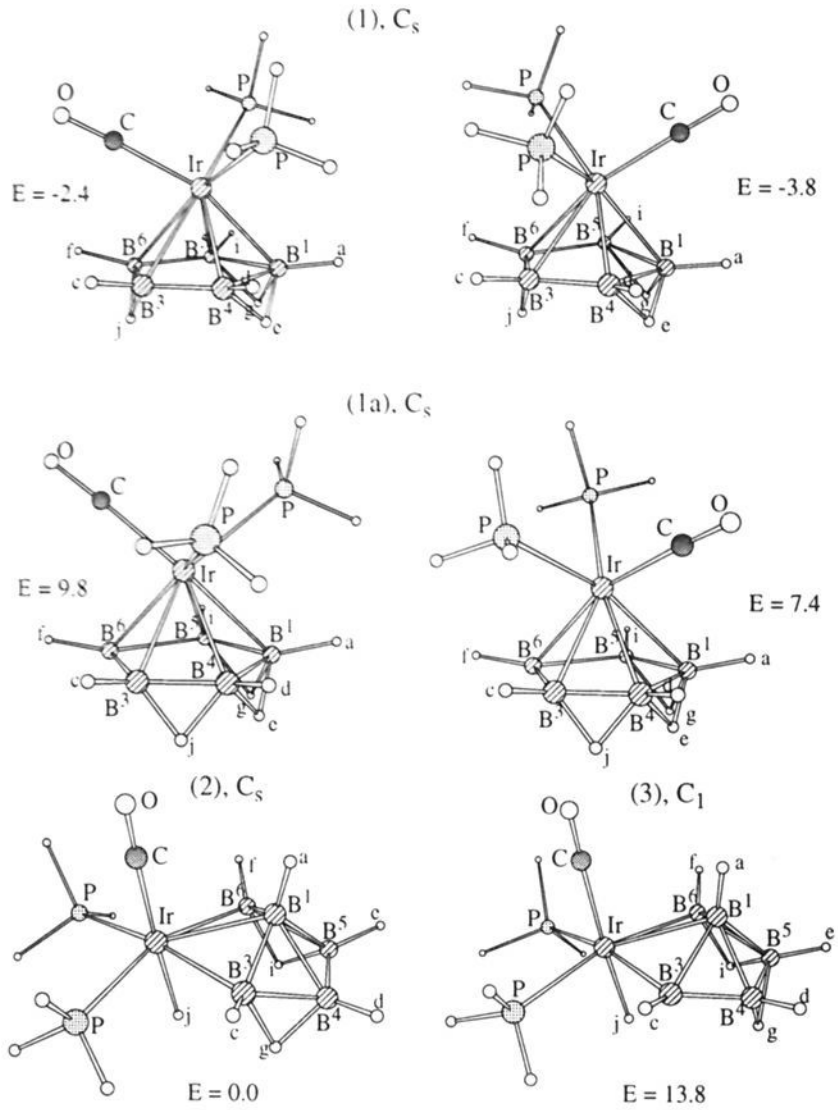

Figure 9. Alternative isomers of $[(IrB_5H_8)(CO)(PH_3)_2]$ and their relative energies (E, kcal/mol) at the MP2//HF/ECP-DZ level.

The calculation indicates that the isomers (1) and (2) are relatively low in energy.[11] While (2) has been observed experimentally,[10] (1) is calculated to be 8.6 kcal/mol lower in energy at the MP4(SDQ) level.[11] The experimental finding of (2) instead of (1) has been explained by the method of synthesis.[10,11] Experimentally the iridaborane was prepared in the reaction

$$K[B_5H_8] + [Ir(CO)Cl(PR_3)_2] \rightarrow KCl + [(IrB_5H_8)(CO)(PR_3)_2]$$

which could proceed by insertion of Ir into a basal B–B bond of the tetragonal pyramidal skeleton of $B_5H_8^-$. The (2) → (1) isomerization process does not occur under normal experimental conditions. We consider here the mechanism of isomerization by calculation of the $C_2(6,0;4,0,0)$-like rearrangement pathway, which is the most favorable for the apical–basal reorganization in the parent B_6H_{10} borane. Before doing so, however, we study processes of bridging hydrogen scrambling in the iridaborane.

A. Bridging Hydrogen Scrambling. Scrambling of a bridging hydrogen along the pyramidal base in B_6H_{10}, which requires an activation energy of 9.4 kcal/mol at the MP2/6-31G*+ZPE level,[13] involves the transition structure containing a BH_2 group with a basal boron atom. We have found similar transition structures, TSH1 and TSH2, shown in Figure 10 and Table 2, for bridging hydrogen migration in the iridaborane. TSH1 corresponds to the barrier between isomers (2) and (3) and involves the B^4H_2 group, with bridging hydrogen H^g transferring from the 3,4 to the 4,5 position. TSH1 lies 14.7 kcal/mol higher than (2) at the MP2 level but only 0.9 kcal/mol higher than (3), indicating the latter would not exist as a stable intermediate. TSH2 connects isomer (1) with (1a). The H^j bridging hydrogen in TSH2 moves from the 3,6 to the 3,4 position. The transition structure is 23.7 and 12.5 kcal/mol higher than the most stable forms of (1) and (1a), respectively. Thus, migration of bridging hydrogens in the iridaborane requires a larger activation energy than in B_6H_{10} but should be possible upon heating.

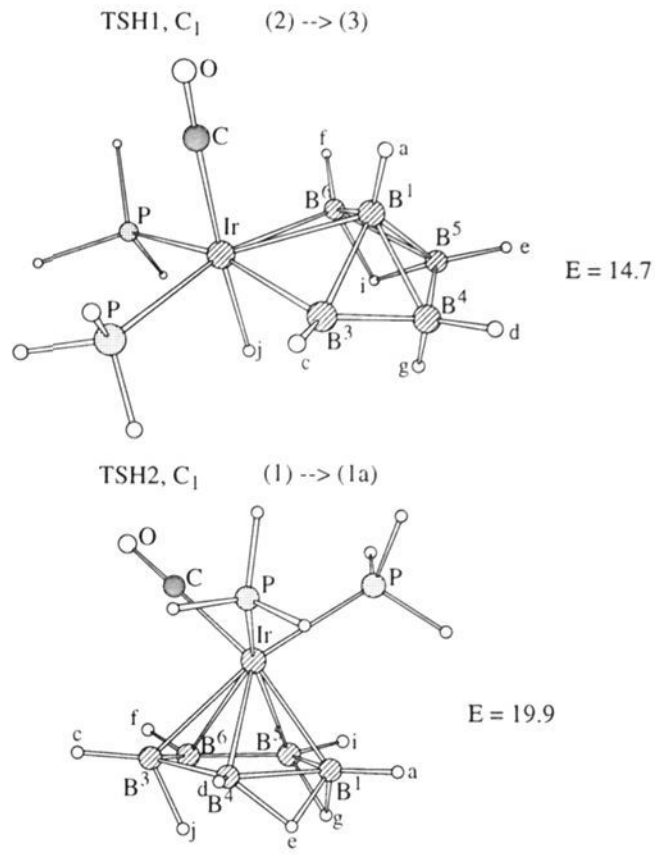

Figure 10. HF optimized geometry of transition structures for bridging hydrogen scrambling in $[(IrB_5H_8)(CO)(PH_3)_2]$. Relative energies (E, kcal/mol) are calculated at the MP2//HF/ECP-DZ level.

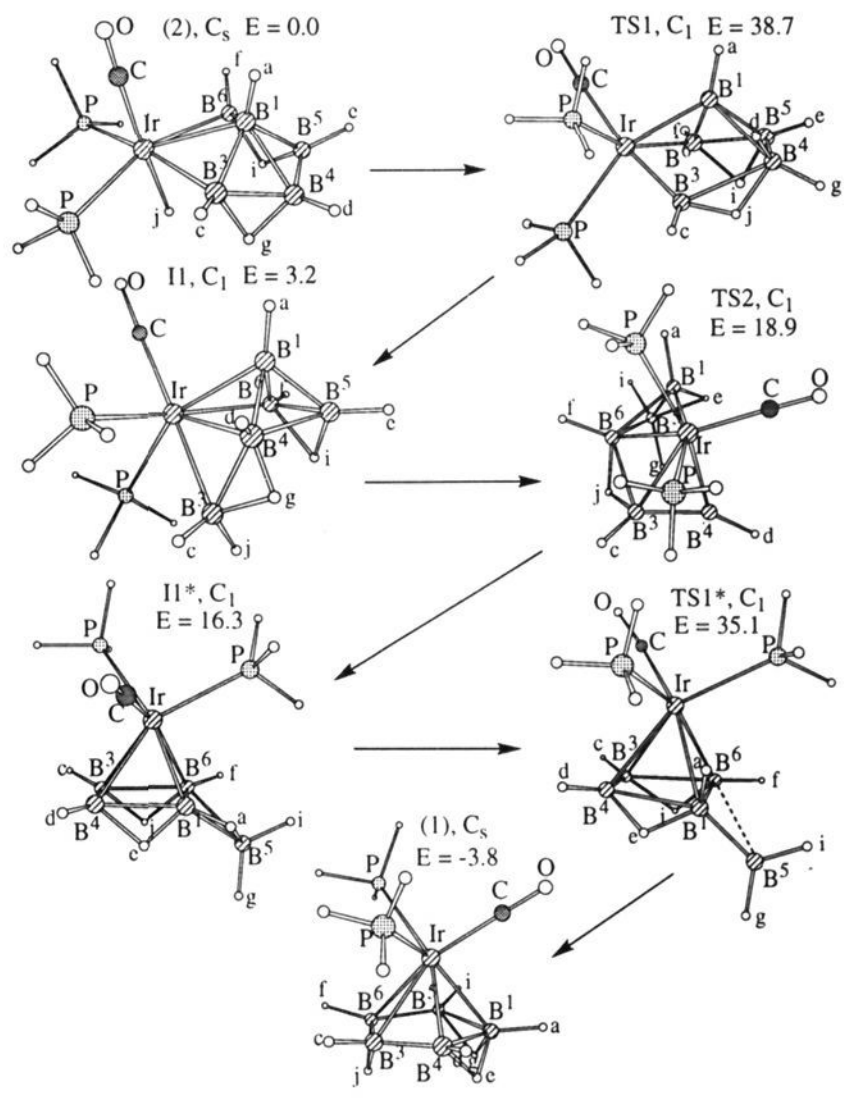

Figure 11. (2) → (1) isomerization mechanism for $[(IrB_5H_8)(CO)(PH_3)_2]$. Relative energies (E, kcal/mol) are calculated at the MP2//HF/ECP-DZ level.

B. Skeleton Rearrangement. The $C_2(6,0;4,0,0)$-like rearrangement mechanism for $[(IrB_5H_8)(CO)(PH_3)_2]$ is shown in Figure 11. As an initial guess for geometry optimization of different structures through the (2) → (1) rearrangement pathway, we used the geometries of corresponding configurations of B_6H_{10}, **TS1**, **I1**, **TS2**, **I1***, and **TS1***, in which one BH group and a bridging hydrogen were replaced by an $Ir(CO)(PH_3)_2$ moiety and distorted to accommodate the larger iridium atom. We maintain in Figure 11 the same atomic labels as in Figure

Table 2. Energies and HF/ECP-DZ Optimized Geometries of Different Configurations of $[(IrB_5H_8)(CO)(PH_3)_2]$[a]

	(2), C_s	(1), C_s	TSH1, C_1	TSH2, C_1	TS1, C_1	I1, C_1	TS2, C_1	I1*, C_1	TS1*, C_1
E_{tot}, au									
HF	−360.459 32	−360.450 60	−360.435 53	−360.413 62	−360.404 53	−360.440 93	−360.426 96	−360.423 16	−360.406 74
MP2//HF	−361.416 22	−361.422 35	−361.392 76	−361.384 54	−361.354 53	−361.411 06	−361.386 14	−361.390 22	−361.360 27
E_{rel}, kcal/mol									
HF	0.0	5.5	14.9	28.7	34.4	11.5	20.3	22.7	33.0
MP2	0.0	−3.8	14.7	19.9	38.7	3.2	18.9	16.3	35.1
IrB^1	2.311	2.303	2.356	2.173	2.150	2.170	2.153	2.083	2.317
IrB^3	2.219	2.348	2.187	2.456	2.089	2.302	2.308	2.322	2.388
IrB^4		2.251		2.274	2.382	2.268	2.119	2.269	2.322
IrB^5		2.251		2.259				3.440	3.806
IrB^6	2.219	2.348	2.216	2.303	2.136	2.148	2.305	2.222	2.115
IrH^j	1.621		1.629		2.987	2.945			
B^1B^3	1.750		1.954		2.634	3.182	3.032		
B^1B^4	1.839	1.907	1.800	1.985	2.128	1.774	2.986	2.021	2.113
B^1B^5	1.839	1.907	1.706	1.915	1.700	1.644	1.738	1.737	1.651
B^1B^6	1.750		1.710		1.815	1.805	1.797	1.820	1.806
B^3B^4	1.740	1.661	1.675	1.646	2.232	1.838	1.640	1.624	1.618
B^4B^5	1.684		1.782		1.800	2.034	3.333		
B^5B^6	1.740	1.661	1.744	1.739	1.735	1.745	2.062	1.980	2.580
B^3B^6		1.840		1.718			1.827	1.911	1.957
B^1H^a					1.181	1.179	1.191	1.249	1.230
B^1H^e		1.302		1.282	2.669	2.618	1.295	1.275	1.329
B^1H^g		1.302		1.320				2.505	2.519
B^3H^g	1.369		2.296		3.010	1.409	3.057		
B^3H^j	2.458	1.319	2.309	1.200	1.267	1.194	1.317	1.352	1.329
B^4H^e		1.339		1.396	2.585	2.922	1.363	1.455	1.355
B^4H^g	1.315		1.249		1.191	1.279	3.047		
B^4H^j				2.498	1.423	2.726	2.471		
B^5H^a					2.502	2.509	2.443	1.514	2.389
B^5H^g		1.339	1.664	1.323	2.459	2.308	1.185	1.184	1.192
B^5H^i	1.315		1.362		1.307	1.283	1.185	1.866	1.196
B^6H^i	1.369		1.331		1.368	1.419	2.861		
B^6H^j	2.458	1.319	2.531	2.564			1.305	1.305	1.321

[a] Bond lengths are in Å; angles are in deg.

3; Ir substitutes B^2 and, since the iridaborane contains only eight "cluster" hydrogens, H^b and H^h disappear in Figure 11. Energies and optimized geometries are collected in Table 2. Since our study on the skeleton reorganization in iridaborane is not as comprehensive as in B_6H_{10}, there may be some additional stationary points between the optimized intermediates and transition structures given in Figure 11 due to additional hydrogen migrations. However, we believe that hydrogen migrations with activation energies of 15–20 kcal/mol are not rate determining steps for the cluster skeleton rearrangement.

The (2) → (1) isomerization process starts from a DSD rearrangement. On going from (2) to TS1, the B^1B^3 bond is broken but the IrB^4 bond is yet to be formed. H^j migrates from the Ir atom to the 3,4 bridging position. On the other hand, H^g leaves the B^3B^4 bridge and becomes a member of the BH_2 group of B^4. The H^i hydrogen remains in the same place. Further, from TS1 to I1, a new IrB^4 bond is formed and the B^3 boron bridges this bond and is located under the basal plane of tetragonal pyramid. Meanwhile, H^j is being included into the BH_2 group of B^3, H^g returns to a B^3B^4 bridging place, and H^i is not involved in the scrambling. I1 is only 3.2 kcal/mol higher than (2) at the MP2//HF level, and the barrier for the DSD rearrangement is 38.7 kcal/mol. This barrier is about 12 kcal/mol lower, without ZPE, than that in B_6H_{10}.

The next step, I1 → TS2, includes migration of Ir into a position above nonplanar base formed by B^3, B^4, B^5, and B^6. B^3 is lifted from under the base into the base. The new B^3B^6 bond is formed. There are some differences between **TS2** of B_6H_{10} and TS2 of $[(IrB_5H_8)(CO)(PH_3)_2]$. In the latter, the B^1B^4 and the B^4B^5 distances appear to be long and nonbonding, while in the former, the B^4B^5 bond breakage occurs later, only in **I1***. H^j from the B^3H_2 group bridges the newly formed B^3B^6 bond, and H^e remains in the terminal place with B^3. H^g transfers from the B^3B^4 bridging position to be included in the B^5H_2 group. This group also contains H^i, which was a bridging hydrogen between B^5 and B^6 in I1. The B^5 terminal hydrogen, H^e, becomes B^5B^1 bridging in TS2. The energy of TS2 relative to (2) is 18.9 kcal/mol, which is much lower than the energy of the corresponding **TS2** in B_6H_{10} or the energy of the first DSD transition state TS1 of the present mechanism.

After this stage, TS2 relaxes into I1*. Similar to I1, I1* is a tetragonal pyramid with two bridging hydrogens and one bridging BH_2, but it contains the apical Ir, whereas I1 contained the basal Ir. From TS2 to I1*, B^1 moves down into the base and B^5 occupies the bridging position under the basal plane. The B^1B^4 bond is formed again, and H^e migrates from the B^1B^5 bond onto this new bond. H^a, the terminal hydrogen on B^1, becomes slightly bound also with B^5. Other hydrogens do not change their connections. The I1* intermediate, with the apical Ir, is 16.3 kcal/mol higher in energy than (2) and is about 13 kcal/mol less stable than I1 with the basal Ir.

Another DSD rearrangement, I1* → TS1* → (1), completes the rearrangement process. As compared with I1*, the B^5B^6 distance is elongated in TS1* to 2.58 Å, comparable with the corresponding distance of 2.70 Å at the HF/6-31G level in **TS1*** of B_6H_{10}, but the B^1B^6 bond is not stretched. Positions of bridging hydrogens do not change, except that H^a is connected again explicitly with B^1. TS1* is an early transition state, in which the B^1B^6 bond will be broken, the IrB^5 bond will be created, the B^5B^6 bond length will shorten back, and H^g will occupy the B^1B^5 bridging position to form product (1). Rotation of the Ir(CO)-$(PH_3)_2$ moiety around the vertical axis is also necessary to get to (1) where the CO ligand is in a cis location relatively B^1. However, the rotation is shown to be almost free. The rearrangement barrier is 18.8 kcal/mol from I1* or 35.1 kcal/mol relative to (2) at the MP2//HF level.

Thus, the highest barrier on the (2) → (1) isomerization pathway, 38.7 kcal/mol, corresponds to the initial DSD rearrangement with the TS1 transition structure. The barrier is significantly lower than that for the degenerate apical–basal

reorganization of B_6H_{10}. It is, however, still very large and can prevent the isomerization even at high temperatures. This high barrier probably explains why the thermodynamically more stable (1) isomer has not been obtained experimentally. Some other synthetic approaches which do not involve formation of (2) could lead to the synthesis of (1). As has been discussed in the Introduction, the (2) → (1) isomerization has been observed experimentally at 175–180 °C for pentagonal pyramidal ferraborane, $[(\eta^5\text{-}C_5H_5)Fe]B_5H_{10}$. Probably, a further decrease in the rearrangement barrier has taken place here.

V. Concluding Remarks

We have performed a systematic study of nearly all possible degenerate cage rearrangement mechanisms in hexaborane(10), B_6H_{10}. All the mechanisms theoretically found to be feasible involve the initial formation of a tetragonal pyramid intermediate $B_5H_8(BH_2)$ via a DSD reorganization. The C_2(6,0; 4,0,0) mechanism, via $B_5H_8(BH_2)$ and a middle structure of C_2 symmetry, has been shown to be most favorable for the apical–basal rearrangement. The C_s(2,4; 4,0,0) pathway, involving migration of the bridging BH_2 group from one basal edge to another in $B_5H_8(BH_2)$ and the middle structure of nido-type with one square open face, is preferable for basal–basal reorganization. For both mechanisms the initial DSD rearrangement is the rate determining step and the barrier is high. Since the mechanism with low activation energy does not exist, degenerate skeleton rearrangements are unlikely to occur for this cluster, in agreement with the absence of their evidence in experiment.[12,14]

The degenerate cluster skeleton rearrangement mechanisms described in this paper for B_6H_{10} may be important for isomerization in related heteroboranes, particularly, in CB_5H_9, $C_2B_4H_8$, $C_2B_4H_7^-$, $C_2B_4H_6^{2-}$, etc., carboranes.[21] For example, two isomers of *nido*-C_2B_4 carborane dianion have been reported, with basal adjacent carbons[24] and with basal carbons apart.[25] However, the isomerization process which might occur by the C_s(2,4; 4,0,0) mechanism has not been observed in these species. Probably, similar to the B_6H_{10} case, the rearrangement barrier is too high.

For $[(IrB_5H_8)(CO)(PH_3)_2]$ iridaborane (2) → (1) isomerization process could proceed by the C_2(6,0; 4,0,0)-like mechanism. The highest barrier on the isomerization pathway also corresponds to the initial DSD rearrangement. While the barrier is significantly lower than that for B_6H_{10}, it is high enough to prevent the isomerization. Alternative synthetic attempts are encouraged to synthesize the unknown (1) isomer with apical Ir.

Acknowledgment. The present research is supported in part by Grants-in-Aid from Ministry of Education, Science, and Culture of Japan. Some numerical calculations were carried out at the Computer Center, Institute for Molecular Science.

(24) (a) Hosmane, N. S.; de Meester, P.; Siriwardane, U.; Islam, M. S.; Chu, S. S. C. *J. Chem. Soc., Chem. Commun.* **1986**, 1421. (b) Siriwardane, U.; Islam, M. S.; West, T. A.; Hosmane, N. S.; Maguire, J. A.; Cowley, A. H. *J. Am. Chem. Soc.* **1987**, *109*, 4600.

(25) Hosmane, N. S.; Jia, L.; Zhang, H.; Bausch, J. W.; Surya Prakash, G. K.; Williams, R. E.; Onak, T. P. *Inorg. Chem.* **1991**, *30*, 3793.